Effect of laser-welding parameters on the heat input and weld-bead profile

K. Y. Benyounis[*], A. G. Olabi and M. S. J. Hashmi

School of Mechanical and Manufacturing Engineering. Dublin City University, Dublin 9, Ireland.

Abstract

Laser butt-welding of medium carbon steel was investigated using CW 1.5 kW CO_2 laser. The effect of laser power (1.2 - 1.43 kW), welding speed (30 - 70 cm/min) and focal point position (-2.5 - 0 mm) on the heat input and the weld-bead geometry (i.e. penetration (P), welded zone width (W) and heat affected zone width (W_{HAZ})) was investigated using Response Surface Methodology (RSM). The experimental plan was based on Box-Behnken design. Linear and quadratic polynomial equations for predicting the heat input and the weld-bead geometry were developed. The results indicate that the proposed models predict the responses adequately within the limits of welding parameters being used. It is suggested that regression equations can be used to find optimum welding conditions for the desired criteria.

Keywords: Laser welding; RSM; weld-bead profile;

1. Introduction

Laser welding has become an important industrial process because of its advantages as a bonding process over the other widely used joining techniques. Laser welding characterize with parallel-sided fusion zone, narrow weld width and high penetration. These advantages came from its high power density, which make the laser welding one of the keyhole welding processes [1]. The laser welding input parameters determine the shape of laser weld bead 'keyhole', due to the combination of these parameters control the heat input [2]. For a good welded quality the combination of the output power, welding speed, focal position, shielding gas and position accuracy should be correctly selected [3]. RSM is widely used to predict the weld bead geometry and mechanical properties in many welding process [4-8]. In this work RSM is used to develop models to predict the heat input and to describe the laser keyhole profile (i.e. weld penetration, welded zone width and HAZ width) for CW CO_2 laser butt-welding of medium carbon steel. The laser input parameters taken into consideration are laser power (LP), welding speed (S) and focused position (F).

2. Experimental design

The experiment was designed based on a three level Box-Behnken design with full replication [9]. Laser power (1.2 - 1.43 kW), welding speed (30 - 70 cm/min) and focal point position (-2.5 - 0 mm) being the laser independent input variables. Table 1 shows laser input variables and experimental design levels used. RSM was applied to the experimental data using statistical software, Design-expert V6. Linear and second order polynomials were fitted to the experimental data to obtain the regression equations. The sequential F-test, lack-of-fit test and other adequacy measures were used in selecting the best models. A step-wise regression method was used to fit the second order polynomial equation 1 to the experimental data and to identify the

[*] Corresponding author. E-mail address: khaled.benyounis2@mail.dcu.ie

relevant model terms [10,11]. The same statistical soft ware was used to generate the statistical and response plots.

$$Y = b_o + \sum b_i \chi_i + \sum b_{ii} \chi_{ii}^2 + \sum b_{ij} \chi_i \chi_j \qquad (1)$$

Table 1.
Process variables and experimental design levels used.

Variables	Code	Unit	-1	0	+1
Laser power	LP	kW	1.2	1.3125	1.425
Welding speed	S	cm/min	30	50	70
Focused position	F	mm	-2.5	-1.25	0

3. Experimental work.

Medium carbon steel with chemical composition in weight percent of 0.46 % C, 0.2% Si, 0.7 % Mn and Fe Balance was used as work piece material. The size of each plate was 180 mm long x 80 mm width with thickness of 5 mm. Trial samples of butt-welding were performed by varying one of the process variables to determine the working range of each variable. Absence of visible welding defects and at least half depth penetration were the criteria of choosing the working ranges. The experiment was carried out according to the design matrix in a random order to avoid any systematic error using a CW 1.5 kW CO_2 Rofin laser provided by Mechtronic Industries Ltd. Argon gas was used as shielding gas with constant flow rate of 5 l/min. Two transverse specimens were cut from each weldment. Standard metallographic was made for each transverse specimen. The bead profile parameters 'responses' were measured using an optical microscope with digital micrometers attached to it with an accuracy of 0.001 mm, which allow to measure in X-axes and y-axes.

The average of two measured weld profile parameters was recorded for each response. The design matrix and the average measured responses are shown below in table 2 and 3.

4. Results and discussion

The results of the weld bead profile were measured according to design matrix table 2 using the transverse sectioned specimens and the optical microscope mentioned earlier, the measured responses are listed in table 3. By feeding the design expert software with this data for analysis. The fit summary output indicates that the linear model is statistically significant for the penetration 'the second response' therefore it will be used for further analysis. While for the other responses the quadratic models are statistically recommended for further analysis.

Table 2.
Design matrix with code independent process variables

Exp. No.	Run order	Laser power kW	Welding speed cm/min	Focused position mm
1	1	-1	-1	0
2	8	1	-1	0
3	13	-1	1	0
4	14	1	1	0
5	4	-1	0	-1
6	16	1	0	-1
7	10	-1	0	1
8	3	1	0	1
9	5	0	-1	-1
10	7	0	1	-1
11	9	0	-1	1
12	6	0	1	1
13	11	0	0	0
14	17	0	0	0
15	2	0	0	0
16	15	0	0	0
17	12	0	0	0

Table 3.
Experimental measured responses.

Exp. No.	Heat input J/cm	P mm	W mm	W_{HAZ} mm
1	1920	3.572	2.358	0.561
2	2280	4.322	2.805	0.872
3	822.857	2.705	1.342	0.392
4	977.143	3.651	1.852	0.384
5	1152	2.655	2.761	0.453
6	1368	3.888	3.381	0.569
7	1152	3.813	2.087	0.511
8	1368	4.539	2.572	0.574
9	2100	3.905	3.681	0.625
10	900	2.367	1.982	0.375
11	2100	4.987	2.423	0.762
12	900	3.824	1.649	0.413
13	1260	3.712	2.625	0.531
14	1260	3.872	2.282	0.562
15	1260	3.586	2.567	0.466
16	1260	3.505	2.413	0.478
17	1260	3.626	2.293	0.506

4.1 ANOVA analysis.

The test for significance of the regression models, the test for significance on individual model coefficients and the lack of fit test were performed using the same statistical package. By selecting the step-wise regression method, which eliminates the insignificant model terms automatically, the resulting ANOVA tables 4-7 for the reduced quadratic models summarise the analysis of variance of each response and show the significant model terms. The same tables show also the other adequacy measures R^2, Adjusted R^2 and predicted R^2. The entire adequacy measures are close to 1, which is in reasonable agreement and indicate adequate models. The adequate precision compares the range of the predicted value at the design points to the average prediction error. In all cases the value of Adequate precision are dramatically greater than 4. The Adequate precision ratio above 4 indicates adequate model discrimination.

From the ANOVA analysis it is clear that for the heat input model. The main effect of the laser power (LP), welding speed (S), the second order effect of welding speed (S^2) and the two level interaction of laser welding and welding speed (LP*S) are the most significant model terms associated with heat input. Secondly for the penetration model, the analysis indicated that there is a linear relationship between the main effects of the three parameters. Also, in case of welded zone width model the main effect of laser power (LP), welding speed (S), focused position (F), the second order effect of welding speed (S^2), the second order effect of the focused position (F^2) and the two level interaction of welding speed and focused position (SF) are significant model terms.

Table 4.
ANOVA table for heat input reduced quadratic model.

Source	Sum of Squares	DF	Mean Square	F Value	Prob > F
Model	3246465	4	811616	11507	< 0.0001
LP	111932.1	1	111932	1587	< 0.0001
S	2880000	1	2880000	40833	< 0.0001
S^2	243952.9	1	243952	3459	< 0.0001
LP*S	10579.56	1	10579	150	< 0.0001
Residual	846.3732	12	70.53		
Cor Total	3247311	16			

$R^2 = 0.9997$ | | | Pred $R^2 = 0.9989$ | | |

Table 5.
ANOVA table for penetration reduced linear model.

Source	Sum of Squares	DF	Mean Square	F Value	Prob > F
Model	6.279	3	2.093	51.399	< 0.0001
LP	1.670	1	1.670	41.007	< 0.0001
S	2.246	1	2.246	55.158	< 0.0001
F	2.363	1	2.363	58.031	< 0.0001
Residual	0.529	13	0.041		
Lack of Fit	0.451	9	0.050	2.560	0.190
Pure Error	0.078	4	0.020		
Cor Total	6.809	16			

$R^2 = 0.922$ | | | Pred $R^2 = 0.849$ | | |
Adj $R^2 = 0.904$ | | | Adeq Precision= 21.931 | | |

Table 6.
ANOVA table for WZ width reduced quadratic model.

Source	Sum of Squares	DF	Mean Square	F Value	Prob > F
Model	5.140	6	0.857	58.732	< 0.0001
LP	0.531	1	0.531	36.440	0.0001
S	2.466	1	2.466	169.105	< 0.0001
F	1.181	1	1.181	80.985	< 0.0001
S^2	0.361	1	0.361	24.750	0.001
F^2	0.386	1	0.386	26.448	0.0004
S*F	0.214	1	0.214	14.666	0.003
Residual	0.146	10	0.015		
Lack of Fit	0.048	6	0.008	0.330	0.891
Pure Error	0.098	4	0.024		
Cor Total	5.286	16			

$R^2 = 0.972$　　　　Pred $R^2 = 0.922$
Adj $R^2 = 0.956$　　　Adeq Precision = 29.498

Table 7.
ANOVA table for HAZ width reduced quadratic model.

Source	Sum of Squares	DF	Mean Square	F Value	Prob > F
Model	0.259	4	0.065	42.631	< 0.0001
LP	0.029	1	0.029	19.138	0.0009
S	0.197	1	0.197	129.953	< 0.0001
F	0.007	1	0.007	4.666	0.0517
LP*S	0.025	1	0.025	16.766	0.0015
Residual	0.018	12	0.002		
Lack of Fit	0.012	8	0.002	0.990	0.5436
Pure Error	0.006	4	0.002		
Cor Total	0.277	16			

$R^2 = 0.934$　　　　Pred $R^2 = 0.861$
Adj $R^2 = 0.912$　　　Adeq Precision = 22.899

However, the main effect of welding speed (S) and the main effect of focused position (F) are the most significant factors associated with the welded zone width. Finally, for HAZ width model it is evident that the main effect of laser power (LP), welding speed (S), focused position (F) and the two level interaction of the laser power and welding speed (LP*S) are significant model terms. However, the main effect of welding speed (S) is the most important factor influent the HAZ width. The final mathematical models in terms of coded factors as determined by design expert software are shown below:

$$\text{Heat input} = 1260 + 118.29 * LP - 600* S + 240* S^2 - 51.43 * LP * S \qquad (1)$$

$$P = 3.68 + 0.46 * LP - 0.53 * S + 0.54* F \qquad (2)$$

$$W = 2.42 + 0.26 * LP - 0.56* S - 0.38 * F - 0.31 * S^2 + 0.30* F^2 + 0.23* S * F \qquad (3)$$

$$W_{HAZ} = 0.53 + 0.06* LP - 0.16* S + 0.03* F - 0.08* LP * S \qquad (4)$$

While the following final empirical models in terms of actual factors:

$$\text{Heat input} = 1380.002 + 2194.28 * LP - 60 * S + 0.6 * S^2 - 22.86 * LP * S \qquad (5)$$

$$P = 0.2162 + 4.061* LP - 0.026494* S + 0.43480* F \qquad (6)$$

$$W = -1.78957 + 2.29111 * LP + 0.060984* S - 0.28628* F - 7.71842E\text{-}004* S^2 + 0.19345* F^2 + 9.25E\text{-}003 * S* F \qquad (7)$$

$$W_{HAZ} = -2.0753 + 2.30778 * LP + 0.038671* S + 0.0238 * F - 0.035444 * LP * S \qquad (8)$$

4.2 Validation of the models.

Figs 1-4 show the relationship between the actual and predicted values of heat input, P, W and W_{HAZ}, respectively. These figures indicate that the developed models are adequate because the residuals in perdiction of each response are minimum, since the residuals tend to be close to the diagonal line. Furthermore, to verify the adequacy of the developed models, three confirmation experiments were carried out using new test conditions, but are within the experiment range defined early. Using the point prediction option in the software, the heat input, P, W and W_{HAZ} of the validation experiments were predicted using the previous developed models. Table 8 summarise the experiments condition, the actual experimental values, the predicted values and the percentages of error.
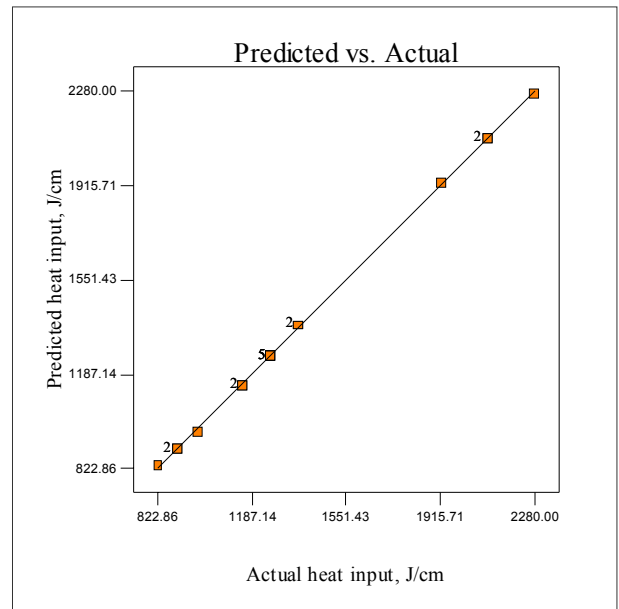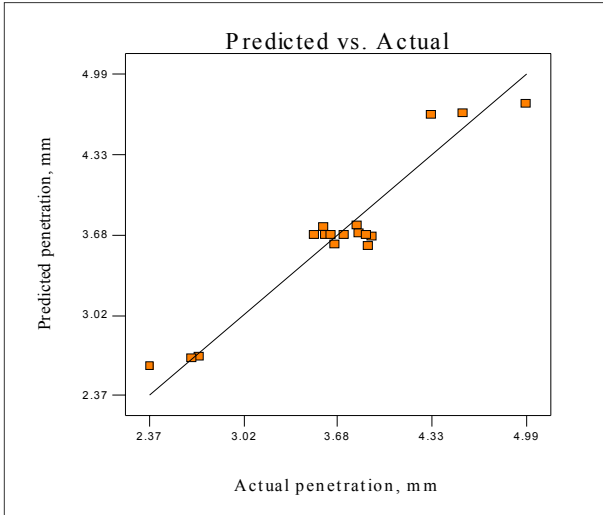

Fig. 1. Scatter diagram of heat input.
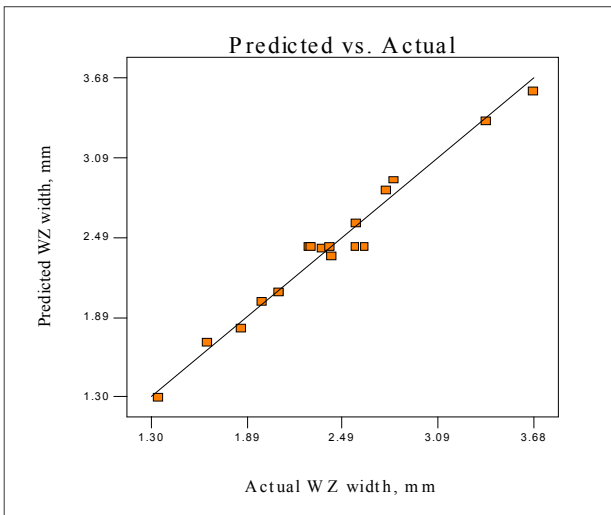
Fig. 2. Scatter diagram of penetration.
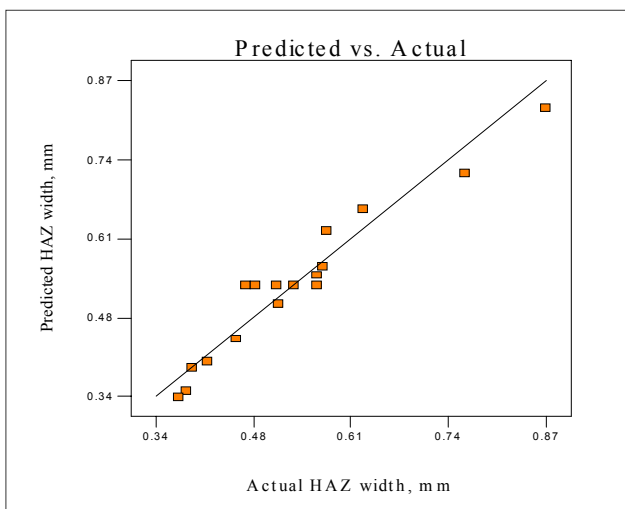

Fig. 3. Scatter diagram of WZ width.

Fig. 4. Scatter diagram of HAZ width.

4.3 Effect of Process Factors on Keyhole Parameters

4.3.1 Heat input

The heat input is directly related to the laser power, the welding speed and welding efficiency. It can be calculated directly from Heat input = (LP/S)*η. Where η is the welding efficiency. The welding efficiency is taking as 80 % [12]. The reason of predicting the heat input is to develop a model to include it into the optimisation step in future work. From figures 5 and 6 it is evident that as the (LP) increases and the (S) decreases the heat input increases.

4.3.2 Penetration.

From the results it is clear that the three parameters are significantly affecting the penetration (P). These effects are due to the following: the increase in (LP) leads to an increase in the heat input, therefore, more molten metal and consequently more (P) will be achieved. However, the idea is reversed in the case of welding speed (S) effect, because the welding speed (S) matches an opposite with the heat input. Using a focused beam results in increasing the power density, which mean the heat will localize in small metal portion resulting in increasing in the power density leading to better (P). To achieve maximum (P) the laser power has to be maximum with focused beam (i.e. F =0) while (S) has to be minimum. Figures 7-10 show the effect of process parameters on the weld penetration.

4.3.3 Welded zone width.

The results indicate that the welding speed (S) and focused position (F) are the most important factors affecting the welded zone width (W). An increase in welding speed (S) leads to a decrease in (W). This is due to the laser beam travelling at high speed over the welding line when (S) is increased. Therefore the heat input decreases leading to less volume of the base metal being melted, consequently the width of the welded zone decreases. Moreover, defocused beam, which mean wide laser beam results in spreading the laser power onto wide area. Therefore, wide area of the base metal will melt leading to an increase in (W) or vice versa. The results show also that laser power (LP) contribute secondary effect in the WZ width dimensions. An increase in (LP) results in slightly increase in the (W), because of the increase in the power density. Figures 11-14 show the effect of process parameters on the WZ width.

4.3.3 Heat affected zone width

The main factor influencing the Width of HAZ (W_{HAZ}) is the welding speed as the results indicated. This is due to the fact that at low (S) the heat input will be greater. This heat will conduct from the fusion zone to the bulk metal through HAZ making it wider and coarser. The results show also that the other two factors and the two level interaction of the (LP*S) are contributing secondary effect in width of HAZ (W_{HAZ}). Figures 15-18 shows the effect of process parameters on the HAZ width.

Table 8.

Confirmation experiments.

Exp. No.	Laser power	Welding speed	Focused position		Heat input	P	W	W_{HAZ}
1	1.35	50	-1.25	Actual	1296	4.012	2.428	0.573
				Predicted	1299.43	3.83	2.505	0.551
				Error %	-0.264	4.75	-3.07	3.99
2	1.31	30	-1.25	Actual	2100	4.407	2.703	0.714
				Predicted	2100	4.21	2.666	0.688
				Error %	0	4.68	1.39	3.78
3	1.31	50	0	Actual	1260	3.962	2.398	0.579
				Predicted	1260	4.22	2.337	0.561
				Error %	0	-6.11	2.61	3.21
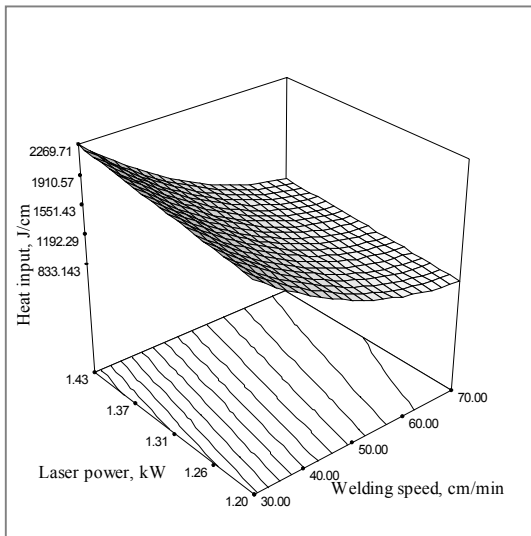
Fig. 5. 3D graph show the effect of LP and S
on the heat input.
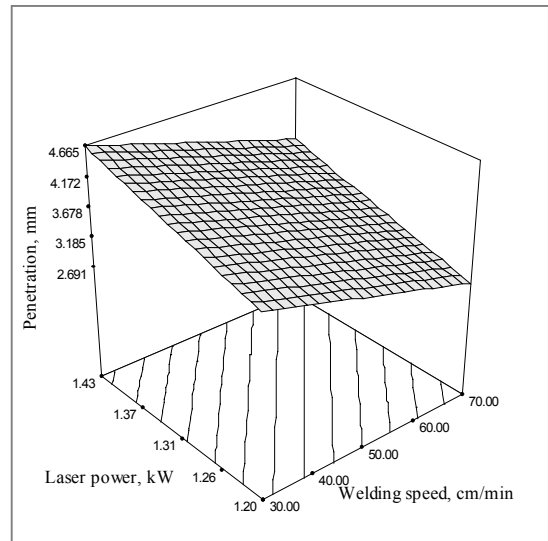
Fig. 7. 3D graph shows the effect of LP and S on
penetration at F = -1.25 mm.
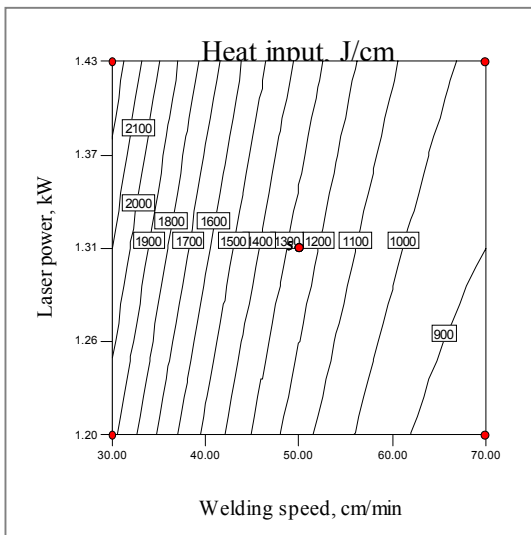
Fig. 6. Contours graph show the effect of LP and S
on the heat input.
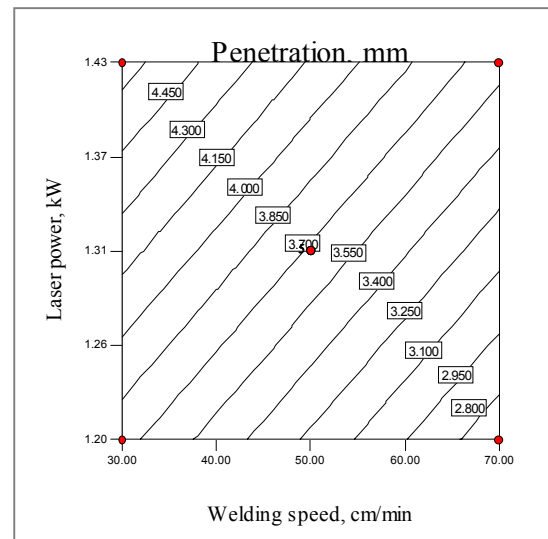
Fig. 8. Contour graph shows the effect of LP and S on
penetration at F = -1.25 mm.
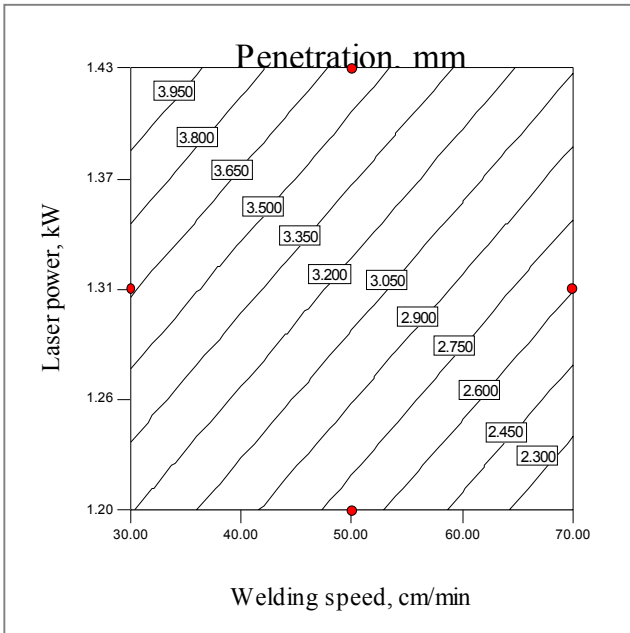
Fig. 9. Contour graph shows the effect of LP and S
on the weld penetration at F= -2.5 mm
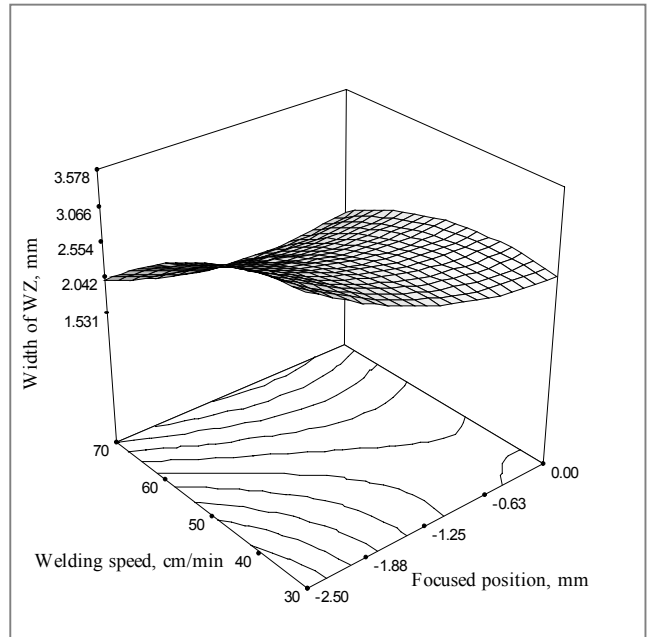
Fig. 11. 3D graph shows the effect of S and F
on the weld width at LP = 1.31 kW.
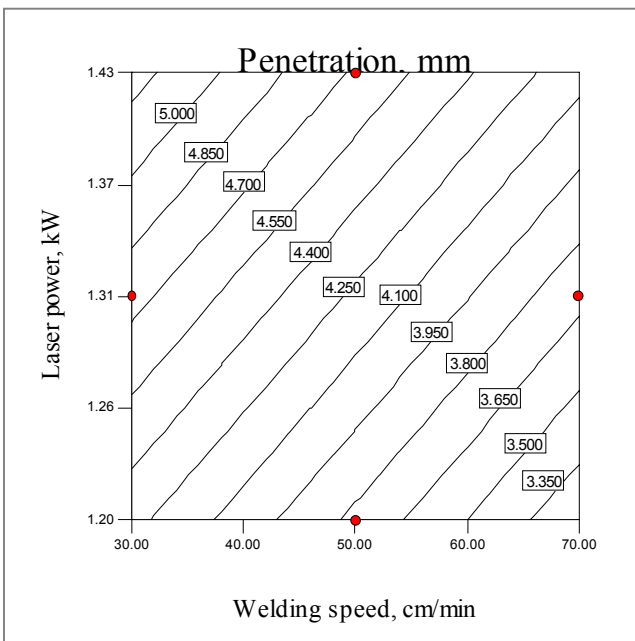
Fig. 10. Contour graph shows the effect of LP and S
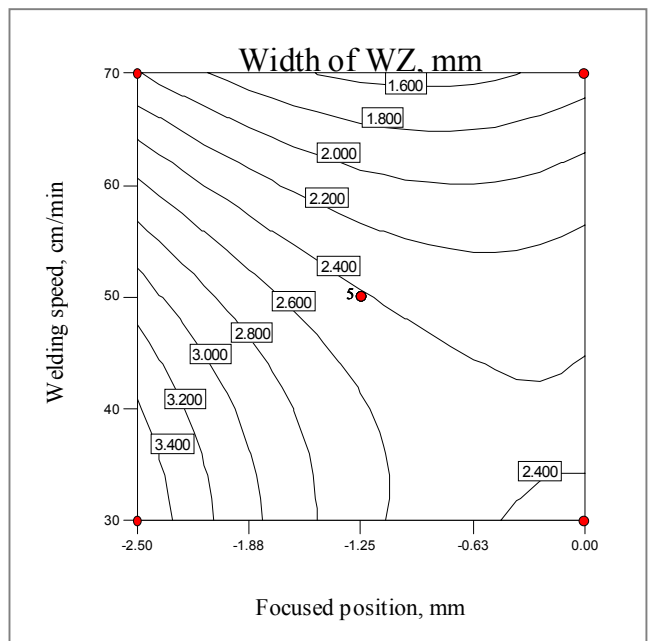on the weld penetration at F= 0 mm

Fig. 12. Contour graph shows the effect of S and F
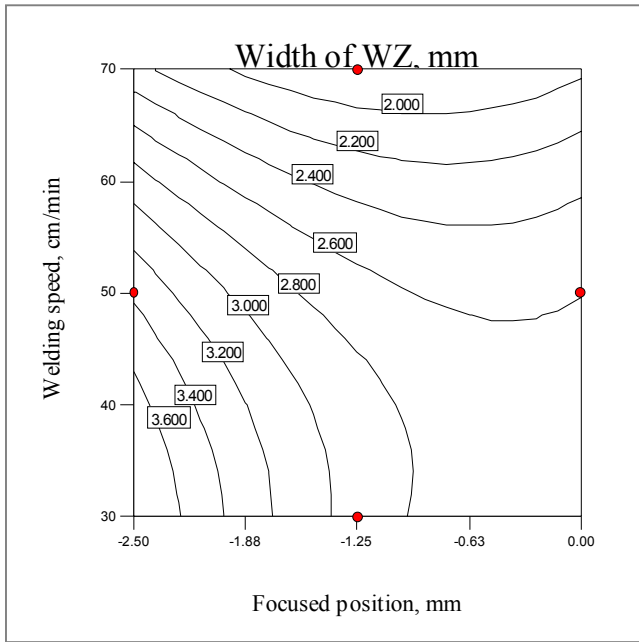on the weld width at LP = 1.31 kW.

Fig. 13. Contour graph shows the effect of S and F on the weld
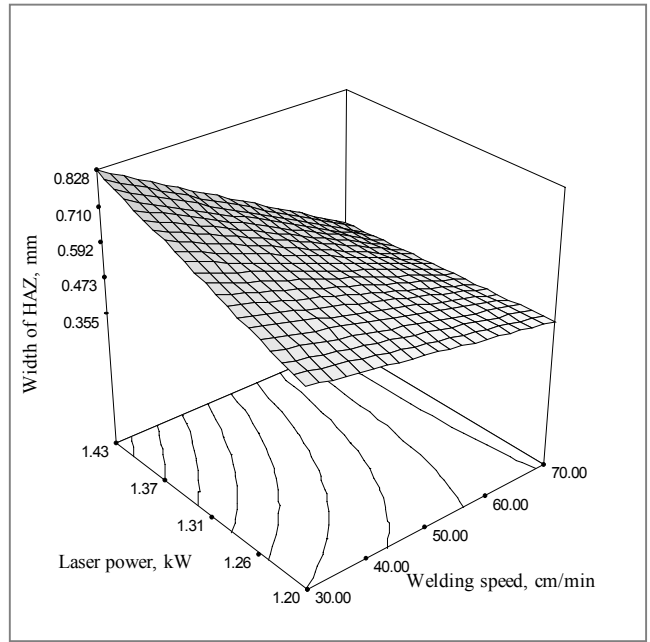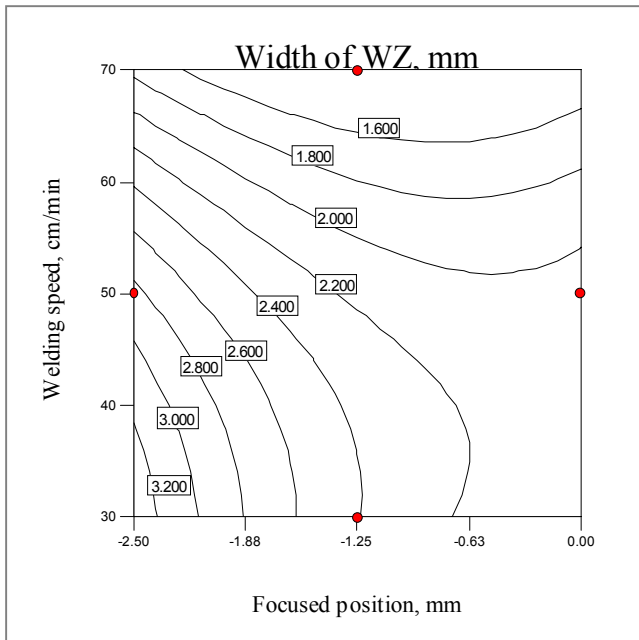width at Laser power= 1.2 kW.

Fig. 15. 3D graph shows the effect of LP and S
on the HAZ width at F = -1.25 mm.

Fig. 14. Contour graph shows the effect of S and F on the weld
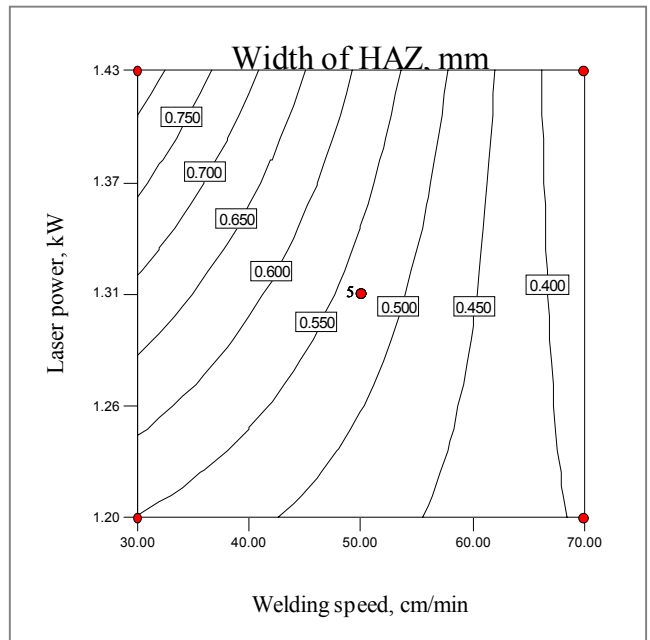width at Laser power= 1.41 kW.

Fig. 16. Contour graph shows the effect of LP and S
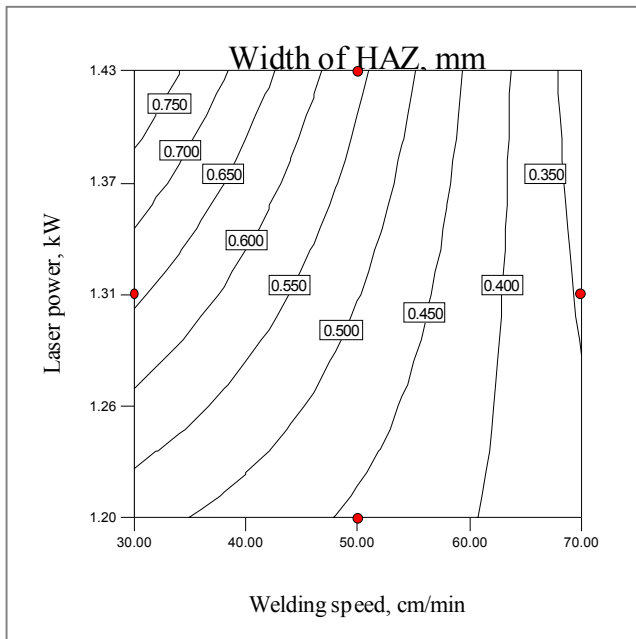on the HAZ width at F = -1.25 mm.

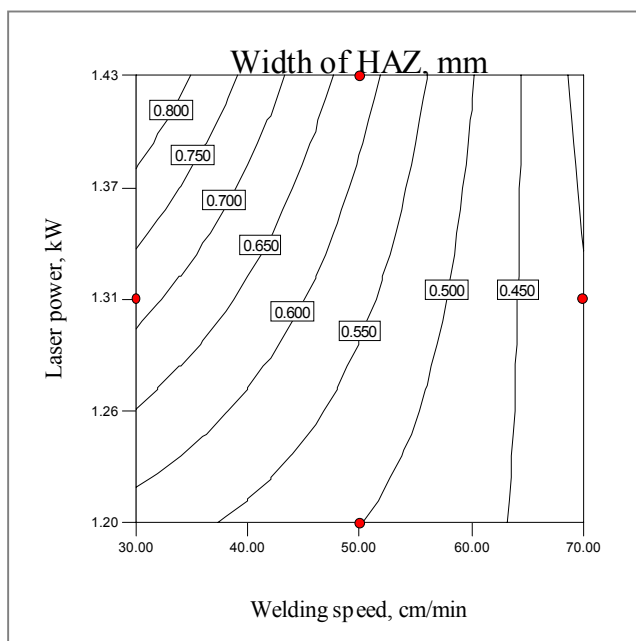Fig. 17. Contour graph shows the effect of S and LP on the HAZ width at focused positions = - 2.5 mm.

Fig. 18. Contour graph shows the effect of S and LP on the HAZ width at focused positions = 0 mm.

5. Conclusion

The following conclusions were drawn from this investigation within the factors limits considered.

1- Box-Behnken design can be employed to develop mathematical models for predicting keyhole geometry.

2- The desired high quality welds can be achieved by choosing the working condition using the developed models.
3- Heat input plays an important rule in the keyhole parameters shape.
4- Welding speed has a negative effect on all the responses investigated whereas; the laser power has a positive effect.
5- As the focused position goes in the metal (F<0) the penetration significantly reduces and the HAZ width slightly reduces, but WZ width increases.

References

[1] W. M. Steen, Laser Material processing, Springer, London, 1991.
[2] C. Dawes, Laser welding, Abington Publishing, New York, NY, 1992.
[3] Q. Huang, J. Hagstroem, H. Skoog and G. Kullberg, Effect of laser parameter variation on sheet metal welding, Inter. J. for the joining of Materials, Vol. 3, No. 3, Sep. 1991, p 79-88.
[4] D. Kim et al, Modelling and optimisation of a GMA welding process by genetic algorithm and response surface methodology, INT. Journal of PROD. RES., Vol. 40, NO. 7, (2002) 1699-1711.
[5] V. Gunaraj and N. Murugan, Application of response surface methodology for predicting weld bead quality in SAW of pipes, Journal of Mater. Processing Technology, Vol. 88, (1999), 266-275.
[6] K.Y. Benyounis, A. H. Bettamer, A.G. Olabi and M.S.J. Hashmi, Predicting the impact strength of spiral-welded pipe joints in SAW of low carbon steel, Proceedings of IMC21, Limerick Ireland, Sep. 2004.
[7] V. Gunaraj and N. Murugan, Prediction of Heat- Affected Zone Characteristics in SAW of Structural Steel Pipes, Welding Journal, American Welding Society, Jan. 2002, p94-s to 98-s.
[8] T.T. Allen, R.W. Richardson, D.P. Tagliable and G.P. Maul, Statistical process Design for Robotic GMA Welding of Sheet Metal, Welding Journal, American Welding Society, May 2002, p 69-s to 77-s.
[9] Design-Expert software, v6, user's guide, Technical manual, Stat-Ease Inc., Minneapolis, MN, 2000.
[10] D.C. Montgomery, Design and Analysis of Experiments, 2nd ed, John Wiley & Sons, New York, (1984).
[11] A. I. Khuri and J.A. Cornell, *Response Surfaces Design and Analysis*, 2nd ed, Marcel Dekker, New York, (1996).
[12] P. W. Fuerschbach, Measurement and Prediction of Energy Transfer Efficiency in Laser Welding, Welding Journal, 1996, Vol. 75, pp. 24s – 34s.